[redacted]

LOS ALAMOS SCIENTIFIC LABORATORY
of the
University of California
LOS ALAMOS • NEW MEXICO

Quarterly Status Report on

Plutonium-238 Space Electric Power Fuel Development Program (U)

October 1-December 31, 1968

UNITED STATES
ATOMIC ENERGY COMMISSION
CONTRACT W-7405-ENG. 36

AEC RESEARCH AND DEVELOPMENT REPORT

[redacted]

Restricted Data

[redacted]

[redacted] in any manner to an unauthorized person is prohibited.

Group 1 - Excluded from automatic downgrading and declassification

[redacted]

This LA...MS report presents the status of the Plutonium-238 Space Electric Power Fuel Development Program of Group CMB-11 of LASL. The previous report in this series, classified Confidential RD is:

LA-4068-MS

This report, like other special-purpose documents in the LA...MS series, has not been reviewed or verified for accuracy in the interest of prompt distribution.

Printed in USA. Charge $0.35. Available from the U. S. Atomic Energy Commission, Division of Technical Information Extension, P. O. Box 62, Oak Ridge, Tenn. 37830. Please direct to the same address inquiries covering the procurement of other classified AEC reports.

[redacted]

Distributed February 3, 1969

LA-4089-MS
C-92a, ISOTOPIC SNAP
M-3679 (60th Ed.)

LOS ALAMOS SCIENTIFIC LABORATORY
of the
University of California
LOS ALAMOS • NEW MEXICO

Quarterly Status Report on

Plutonium-238 Space Electric Power Fuel Development Program (U)

October 1-December 31, 1968

to

Space Isotopic Fuels and Materials Branch

Space Electric Power Office

Division of Space Nuclear Systems

[redacted]

[redacted]

UNCLASSIFIED

PROGRAM 07433

PLUTONIUM-238 SPACE ELECTRIC POWER FUEL DEVELOPMENT

Person in Charge: R.D. Baker

Principal Investigator: J.A. Leary

I. INTRODUCTION

A. Properties of solid solutions and possible advantages

In order to gain some insight into what is meant by a solid solution fuel, it would be helpful to describe its structure.

Consider a simple crystallographic lattice array of plutonium and oxygen atoms. In the case of PuO_2, the plutonium atoms are located in a face-centered cubic array. A plutonium atom can be removed from the crystal lattice, and its position can be filled by substituting a diluent atom such as zirconium or thorium. This substitution can be continued until a large fraction of the plutonium atoms has been replaced. The diluent atom will be larger or smaller than the plutonium atom, so some expansion or contraction of the crystallographic unit cell will occur. However, as long as the crystal habit remains unchanged, one has a solid solution of the diluent atom oxide in PuO_2. In some systems there is only limited solubility, while in others the solubility is very extensive.

For this application diluents that have very high solubilities were selected. Moreover, the diluents were chosen to enhance the properties of the PuO_2. For example, diluents having oxides that are more stable than PuO_2 were selected so that the resulting solid solution would be more stable than PuO_2. The free energies of formation of these diluents are more negative than that of PuO_2. The following properties of such solid solutions may be predicted on the basis of known thermodynamic correlations:

1. The thermal stability of the PuO_2 is increased. Thus the tendency for PuO_2 to dissociate or vaporize is reduced. Moreover, the melting point can be increased.

2. The power density of a given fuel body can be varied over a significant range with minimal change in fuel properties.

3. By judicious choice of diluent the reactivity of PuO_2 with water and with container materials can be reduced.

4. The specific radioactivity of a given size respirable particle of PuO_2 is reduced.

In addition to these possible advantages, the process for making solid solution fuels is relatively economical. It consists of simply blending unshaped PuO_2 and diluent oxide powders, followed by cold pressing and sintering. It should be noted that it is not necessary to melt the fuel in order to prepare a solid solution; the solution is formed by a solid state diffusion during the sintering process.

B. The overall program

The first task in the program was to conduct an accelerated short-term development phase to provide a technical basis for estimating the performance of $^{238}PuO_2$ solid solution fuels by November, 1968. This included

[redacted]

process chemistry development, fabrication development, properties measurements, and theoretical estimates of performance of various fuel compositions and various power densities.

The second task involves follow-on fabrication and properties work with the preferred fuel composition for the purpose of establishing the capability for producing a limited number of large specimens for use as heat sources.

The later tasks in the program are directed towards defining production methods and economics, and to provide assistance to the Commission and its contractors in order to establish a reliable commercial capability.

II. RESULTS AND CURRENT STATUS

A. Large disc fabrication development

General procedures and flowsheet were described in the last report. The goal of this quarter was to (1) demonstrate fabrication capability for and (2) to prepare a limited number of nominally 2 in. dia discs. The composition of the discs was to be determined by the power density required. In turn the power density was affected primarily by the Pu concentration and the pellet sintered density.

Efforts toward standardization of procedures were started and completed for PuO_2-$ZrO_2|Y|$ compositions. The following procedure was found to produce satisfactory discs:

1. Individually grind PuO_2 and diluent followed by screening to $\leq 44\mu$ size
2. Blend the PuO_2 and diluent followed by screening to $\leq 44\mu$ size
3. Cold compaction at 7.5 tsi pressing pressure with the use of 1 w/o paraffin binder
4. Sinter at 1625°C for 6 hrs in CO_2
5. Products are characterized by dimensioning, weighing, x-ray powder diffraction analysis, chemical analysis, quantitative spectrochemical analysis, and metallographic examination of destructive product sampling or by sampling companion pellets.

Current Results

Several large discs of $^{238}PuO_2$-ZrO_2 were prepared as shown in Table I. The discs were of good integrity with no detectable cracks. Metallographic examinations of $^{239}PuO_2$-ZrO_2 control specimen indicated a small amount of grey phase and trace of a metallic appearing phase, similar to that found previously in $ZrO_2|Y|$ solid solutions. Typical spectrochemical analysis shown in Table II indicate that the impurity levels in the PuO_2-$ZrO_2|Y|$ solid solution materials are mainly derived from the impurities in commercially supplied $ZrO_2|Y|$. The purity of plutonium powders used was tabulated in the last report.

Fabrication development of the large PuO_2-ThO_2 solid solution discs also has been started.

The particle size distributions of powders used in this program were determined by a sedimentation method using a Sartorius Sedibal. Results are summarized in Table III.

B. Small test specimen fabrication development

In some applications the maximum attainable power density is required of PuO_2 fuels. Therefore one lot of twenty $^{239}PuO_2$ pellets was prepared by the method described in the previous section.

The average density of the 14 pellets was 98.2 ± 0.2 percent of theoretical, as shown in Table IV. This would correspond to a power density of 4.53 watts/cc if the conventional 80 atom percent ^{238}Pu were used. The average diameter was 0.2444 ± 0.0007 in. (deviations are ± 2σ). Thus very dense pellets can be fabricated reproducibly.

Six companion pellets are being subjected to destructive evaluation by chemical analysis, metallography, x-ray powder diffraction, etc. Preliminary results indicate single phase PuO_2 with a lattice dimension of 5.3950 ± 0.0004 A, having a small amount of uniformly distributed porosity.

Chemical composition of the PuO_2 powder used to fabricate these pellets is shown in Table V.

C. Microstructures of ^{238}Pu fuel materials

Metallographic and electron microprobe examination have been completed on the $^{238}PuO_2$, $^{238}PuO_2$-ThO_2, and $^{238}PuO_2$ specimens prepared previously. Photomicrographs are shown in Figures 1, 2, and 3. In addition, emission spectrochemical analyses on these specimens

are shown in Table VI.

As shown in Figure 1, the fuel and porosity distributions in $^{238}PuO_2$ pellet T-10-91-2 were very uniform. Electron microprobe examination indicated a uniform distribution of Pu, with no intergranular impurities.

The $^{238}PuO_2$-ThO_2 solid solution specimen is shown in Figure 2. This high geometric density corresponds to a power density of 1.8 watts/cc at this composition. Electron microprobe examination indicated that the plutonium and Th x-ray intensities varied by not more than 5 percent across the grains. The relative standard deviations for measuring Pu and Th intensities are 1.0 and 1.9 percent, respectively. A sample of this same pellet was examined by x-ray powder diffraction analysis. The material was found to be single phase fluorite structure having a lattice parameter of 5.5114± 0.0005 A, which is in excellent agreement with the Vegard's Rule plot shown in the previous report. Chemical analysis of this specimen was 49.3% by wt. Th found, compared to 49.2% by wt. added; 39.3 ± 0.4% by wt. ^{238}Pu found, compared to 38.8% by wt. added.

The microstructure of $^{238}PuO_2$-$ZrO_2|Y|$ pellet T-10-120-10 reflects the relatively high (~ 0.2% by wt.) impurity level that is traceable to the commercial $ZrO_2|Y|$ powder. Electron microprobe examination showed that the ^{238}Pu and Zr were uniformly distributed in the $(Pu, Zr)O_2$ phase, both within individual grains and from grain to grain. The high Si impurity content in the ZrO_2 resulted in a significant volume fraction of grain boundary impurity phase that contained mainly Si, Ca, and O. Apparently the 4.8% by wt. of CaO present in stabilized ZrO_2 powder is fluxed by the Si impurity. Chemical analysis of this specimen indicated 58.5% by wt. ^{238}Pu, 22.7% by wt. Zr, and 1.33% by wt. Ca; the as added composition was 57.3% ^{238}Pu, 23.7% Zr, and 1.20% Ca.

It should be emphasized that small amounts of light element impurities on a weight basis can amount to very large amounts on an atomic basis in heavy element compounds such as PuO_2. For example, one percent by weight of either B, Na, Mg, Al, or Si corresponds to 20, 11, 10, 9, and 9 atom percent respectively in PuO_2.

In order to evaluate the true properties of PuO_2-$ZrO_2|Y|$ solid solutions, a better purity ZrO_2 powder is being sought.

D. Compatibility

1. Fabrication of new specimens: The high temperature (1600-1800°C) compatibility test specimens must be shorter than the 0.25 in. tall pellets used in the normal 900°C compatibility test capsules. Therefore the twelve short pellets described in Table VII were fabricated by the standard procedure during this quarter. Four pellets each of $^{238}PuO_2$, $^{238}PuO_2$-ThO_2, and $^{238}PuO_2$-ZrO_2 were prepared. Even with these thin wafers, the sintered specimen diameters were quite reproducible for each composition, as were the sintered densities. Spectrochemical analyses of the powders used to prepare these specimens are shown in Table VIII.

2. Compatibility test capsules: In the previous report the 900°C test capsule design and experimental procedures were described. Results of the first test of TZM with PuO_2, PuO_2-$ZrO_2|Y|$ solid solution, and $ZrO_2|Y|$ after 744 hr at 900°C were discussed. There was no evidence of interaction between any of the materials. A companion capsule having the same components has been in test at 900°C for over 2000 hr.

A second group of three compatibility capsules has been in test for 200 hrs at 900°C. TZM is again the metallic member of the compatibility couple and the ceramics include ThO_2; 47 w/o PuO_2 - 53 w/o ThO_2 (1.7 watt/cc); PuO_2; ZrO_2; 65 w/o $^{238}PuO_2$ - 35 w/o ZrO_2 (1.7 watt/cc); and 93 w/o $^{238}PuO_2$ - 7 w/o ZrO_2 (3.5 watt/cc). After a minimum of 1000 hrs exposure at 900°C these couples will be evaluated metallographically.

Assemblies for testing of solid solution fuels in contact with TZM at temperatures of above 1500°C have been designed and produced. Fuel pellets are available and loading will proceed early in January.

E. Helium release

The $^{238}PuO_2$, $^{238}PuO_2$-ThO_2, and $^{238}PuO_2$-$ZrO_2|Y|$

pellets that have been in storage accumulating He have been transferred to the mass spectrometer test area and measurements will be started in January.

F. Thermal diffusivity

Thermal diffusivity measurements on $^{238}PuO_2$-$ZrO_2|Y|$ specimens G-520-2 (85 m/o PuO_2) and G-520-4 (45 m/o PuO_2) have been completed by BMI/PNL over the temperature range 100-1600°C. These specimens are to be returned to LASL for destruction and confirmation of composition, density, and microstructure. Based on the calculated geometric densities, which are probably lower than the true densities, the thermal diffusivities are in fairly good agreement with those predicted for these materials and published in the data sheets, as shown in Table IX. Only the values at 700 and 1200°C are compared in this Table, as only these two temperatures were used as illustrations in the data sheets. However, the PNL measurements were done over the complete temperature range 100-1600°C.

Additional thermal diffusivity specimens of $^{238}PuO_2$ and $^{238}PuO_2$-ThO_2 solid solution that have been prepared this quarter and shipped to PNL are listed in Table X. The geometric densities shown in this table are provisional, and probably are low. True densities will be determined accurately after thermal diffusivity measurements are completed.

The true densities of companion wafers are shown in Table XI. These are determined by weighing the specimens in air, then coating with a thin film of plastic, and reweighing in water. After making the small correction for the volume of plastic, the true density was calculated in the standard Archimedean way.

Spectrochemical analyses of the $^{238}PuO_2$, and ThO_2 starting powders are compared with that of the ThO_2 - 44 w/o $^{238}PuO_2$ sintered specimens in Table XII.

G. Solubility of solid solution fuels in sea water

In the last quarterly report the dissolution rate of ^{238}Pu in 0.1 N H_2SO_4 was compared for plasma torch microspheres and solid solution pellets. The rate of dissolution of ^{238}Pu from the solid solution was 1/700th that from microspheres on a weight basis, and 1/25th that from microspheres on a specific surface area basis.

During this reporting period the relative dissolution rates in sea water were compared in the following experiment. Samples of plasma torch $^{238}PuO_2$ microspheres (lot MLM-72) and a $^{238}PuO_2$-ThO_2 pellet (no. T-10-127-9, 1.7 watts/cc) were first cleaned ultrasonically to eliminate any fines, then placed in 250 ml of Standard Sea Water P_{44} from Charlottenlund Slot, Denmark. The microspheres weighed 8.9 mg, and had an approximate surface area of 31.5 sq. mm. The pellet weighed 1.9819 g, and had a surface area of 188.8 sq. mm. The sea water was slowly and continuously stirred, and aliquots were removed periodically. Each aliquot was filtered through a 5μ millipore filter and analyzed radiochemically for ^{233}Pu. The "dissolution rates" were calculated from four analyses on each sample. Results for the first 144 hr of contact are shown in Table XIII.

The dissolution rates were 3.9 μg/g/hr and 2.9×10^{-4} μg/g/hr for the microspheres and solid solution fuel, respectively. Thus, on a weight basis, the solid solution fuel dissolved at a rate that was 0.74×10^{-4} that of the microspheres. Referred to an area basis, the rates were 1.1×10^{-3} and 3×10^{-6} μg/sq. mm/hr for the microspheres and the solid solution fuel, respectively. Thus, on an area basis, the rate of dissolution of the solid solution fuel was 2.7×10^{-3} that of the microspheres. On either basis, the dissolution rate of the solid solution fuel was orders of magnitude less than that of the microspheres.

Analyses of the sea water above the microspheres after the first six days showed that the "dissolution" rate leveled off, and the concentration of ^{238}Pu remained essentially constant at 0.092 μg/sq. mm. in the 250 ml volume for at least 15 days. After the first six days, the apparent "dissolution" rate of ^{238}Pu from the pellet decreased to 9.2×10^{-7} μg/sq. mm./hr and remained essentially constant at this level for 15 days.

H. Mechanical properties

1. Compression and Bend Testing: Right circular

cylinders of ZrO_2 1/4" dia x 1/4" long and 2" dia x 1/2" long have been prepared for use in developing compressive and diametral mechanical test techniques to be used on fuel compositions. An electro-optical strain measuring device will be utilized, at least during the technique development stage.

A subpress for aligning the compressive load of the Instron tester has been order, and samples are in fabrication. These include plutonia, plutonia-zirconia, and plutonia-thoria right circular cylinders having the same dimensions as the zirconia samples mentioned above.

2. Impact testing

The second impact capsule was examined after being impacted by the Sandia Corp. The impact velocity was 158 fps and the target consisted of an assembly of lead cones designed to provide a negative acceleration of 10,000 G's. Metallographic examination of eight sections cut from the weld area after the impact revealed the presence of small cracks extending about one fifth of the distance from the root of the joint toward the surface of the weld bead. These cracks were intergranular in the martensitic material of the bead. Although the cracks were not present in the weld of the first capsule (not impacted), it is not clear whether they were caused by the impact or represent a welding defect not present in the first unit. The cracks, however, do not appear to be detrimental to the use of such containers for impact testing of plutonium-bearing fuel materials.

Two additional capsules, both containing ZrO_2 discs, were welded and sent to Sandia for impacting. These units will be used to check the procedures for evaluating particle sizes of Pu-bearing fuels after impact. (This work is being carried out as a part of the Advanced Safety Technology Program.) Impact testing of the PuO_2 solid solution specimens is scheduled for mid-January.

I. Specimens for SEPO/Safety tests

The samples shown in Table XIV have been delivered during the past quarter for safety evaluation.

II. FUNDAMENTAL STUDY OF HELIUM RELEASE

A. Bubble formation

The first use of the Van de Graaf accelerator for alpha bombardment of ThO_2 was on December 24. During the 8-hr shift, much of the time was spent in getting the accelerator tuned and aligned. One sample was bombarded briefly that day, but the current (helium ion deposition rate) could not be determined because of peculiarities related to the insulating nature of the sample.

The accelerator was used again on December 31. This time, current readings were made with the beam striking the copper target plate and then a ThO_2 sample was put into place. Bombardment at 9 MeV and 0.55 μA overheated the Havar foil and resulted in burn-through. (The foil absorbs 4 MeV, so that the sample receives the desired 5 MeV particle energy.) After the foil was replaced, a ThO_2 sample was bombarded for 1 hr 50 min at $\sim$ 0.275μA. This resulted in a calculated formation of $\sim$ 0.3 a/o helium in the deposition zone of the sample. The disc is being examined metallographically to see if it suffered visible damage due to exposure. Fortunately, residual radioactivity in these samples after bombardment is negligible (< 1 mR/hr).

Several minor modifications have been made in the test chamber as a result of experience gained to date. Thirty additional ThO_2 discs have been ordered with delivery expected about February 15. Since the accelerator will be shifted from the desired tandem configuration early in March, 1969, careful planning will be necessary in order to complete the bombardment schedule by that time.

B. Release studies

Studies of helium release from $^{238}PuO_2$ have been started. The technique consists of measurement of the helium release rate from a sample with the quadrupole mass spectrometer. In order to permit analysis of the data, only one measurement at constant temperature is done for each sample. The sample is raised rapidly to the chosen temperature and release rate is monitored continuously as a function of time. After the isothermal release has been observed for a sufficient time, the

temperature is raised so as to remove all the helium stored in the sample. Integration of the entire release rate–time plot yields the total helium content of the sample. Using this total content together with the isothermal rate curve, it is possible to compute the fraction of helium released at any time. Results thus consist of fraction released as a function of time.

As a first approach, it is assumed that the process of helium release from microspheres is that of pure bulk diffusion from a sphere. The initial concentration of helium is taken as uniform throughout the sphere (i.e. at $t = 0$, $C = C_o$). The differential equation is

$$\frac{\partial C}{\partial t} = D\left(\frac{\partial^2 C}{\partial r^2} + \frac{2}{r}\frac{\partial C}{\partial r}\right)$$

where C is concentration and D is the diffusion coefficient. The boundary condition is for free vaporization at the surface ($r = a$). An exact solution for the fraction released at any time t is:

$$F = 1 - 6 \sum_{n=1}^{\infty} \frac{(ah)^2}{\beta_n^2\left(\beta_n^2 + ah\,(ah-1)\right)} \exp\left(-\beta_n^2\, Dt/a^2\right)$$

where ah is a dimensionless parameter which comes from the boundary condition and essentially characterizes the relationship of vaporization rate, sphere diameter and diffusion rate. The β_n are roots of the equation $\beta_n \cot \beta_n + ah - 1 = 0$. As ah becomes large, β_n approaches $n\pi$. Calculation of the free vaporization rate for helium shows that ah is sufficiently large so that the solution reduces to:

$$F = 1 - \frac{6}{\pi^2} \sum_{n=0}^{\infty} \frac{1}{n^2} \exp\left(-n^2\pi^2\, Dt/a^2\right)$$

which is also the solution for the boundary condition of surface concentration equal to zero. Dt/a^2 is a dimensionless number which characterizes the process. A "universal" curve of F vs Dt/a^2 may be computed for various values of Dt/a^2. Having this curve, for a given observed value of F, the corresponding value of Dt/a^2 may be found, and D/a^2 may be found from the observed t. The process is actually carried out by interpolation in a table of F vs Dt/a^2 generated by the computer. Thus a value for D/a^2 is found for every experimental point and since each point has a time associated with it, a plot of D/a^2 vs time at constant temperature is obtained for each experiment. The sphere radius is a, for the present it seems appropriate to use D/a^2 rather than to insert the geometric radius of the microspheres; a is then considered an "effective radius" which may or may not correspond to the geometric radius.

If the above model applies, that is if bulk diffusion is the process, then D/a^2 should be constant with time.

Results obtained to date from three experiments show that D varies with time, increasing rapidly at first, passing through a maximum then decreasing. The maximum range of D/a^2 has been less than a factor of 2.

A summary of the results is given in Table XV.

A number for the total helium inventory for the samples has not yet been calculated. This particular lot of microspheres is about 2 years old, and thus should contain about 1 cm^3 (STP) of helium per gram of PuO_2.

C. X-ray line broadening analysis

The computer program which will be used to analyze the self-damage caused by alpha-irradiation and helium storage has been debugged and improved. Equations for determining the standard deviations on the observed and reference Fourier coefficients have been inserted and the errors have been propagated through the remainder of the program to yield the standard deviations of the Fourier coefficients representing the unfolded or deconvoluted line shape.

[redacted]

Table I

Characteristics of Large Fuel Discs (PuO_2-ZrO_2|Y|)

Disc No.	Nominal w/o Pu	Product w/o Pu	Pu Isotope	Product: Calculated Density, g/cc	Product: Dimensions, in. L.	Product: Dimensions, in. Dia.	Product: Equivalent Power Density, w/cc	Product: Lattice Dimension Å
7-111-1B	59.5	57.2	239	6.9(a)	0.450	1.79	1.63	5.239
7-114-1A	60.8	60.8	239	6.9	0.436	1.79	1.69	5.245
7-114-B	60.8	60.8	239	7.01	0.285	1.804	1.71	5.245
7-115-1	62.2	···	238	6.9	0.281	1.75	1.73	5.243(b)
7-122-1	62.2	···	238	7.4	0.258	1.753	1.85	···

Notes: (a) From dimensions and weight. Normally gives a value that is a few percent low.
(b) Corrected for self-irradiation damage.

Table II

Spectrochemical Analysis of Typical PuO_2-ZrO_2|Y| Disc

Element	Concentration(a) disc	Concentration(a) ZrO_2 Powder	Element	Concentration disc	Concentration ZrO_2 Powder
Li	1	···	Zn	< 10	< 30
Be	< 1	< 1	Ni	< 10	10
B	< 1	< 3	Cu	< 10	30
Na	15	200	Sr	200	···
Mg	300	50	Nb	100	< 300
Al	30	1000	Mo	< 30	< 100
Si	1000	5000	Ag	< 1	···
Ti	150	100	Cd	< 3	···
V	< 30	50	Sn	< 1	< 30
Cr	30	50	Ba	20	···
Mn	< 10	50	Pb	< 3	< 30
Fe	400	400	Bi	< 1	< 3

Note: (a) ppm by wt.

Table III

Particle Size Distribution of Typical Oxide Powders (After Ball-Milling)

Lot No.	Oxide	MMD,[a] μ	w/o Greater Than 2μ	5μ	10μ	15μ
MWS-1	ZrO_2	4.6	80	46	15	4
WCP-1	ThO_2	1.7	30	10	3	1
MWS/RLN-1	$^{239}PuO_2$	2.0	50	13	6.5	4
WCP-LA-520102	$^{238}PuO_2$	1.7	37	24	19	13

[a] Mass Median Diameter

Table IV

Characteristics of 100 Percent $^{238}PuO_2$ Pellets

Pellet no.	Wt, g	Dia, in.	Length, in.	Immersion Density, g/cc	% Theoretical Density
T-10-150-5	2.2809	0.2438	0.2678	11.24	98.1
-10	2.1687	0.2445	0.2543	11.24	98.1
-11	2.1750	0.2443	0.2557	11.25	98.2
-12	2.4964	0.2443	0.2934	11.23	98.0
-13	2.1665	0.2449	0.2535	11.26	98.2
-14	2.1364	0.2448	0.2503	11.25	98.2
-15	2.1723	0.2449	0.2553	11.28	98.4
-16	2.1696	0.2443	0.2543	11.25	98.2
-17	2.1790	0.2445	0.2566	11.27	98.3
-18	2.1723	0.2444	0.2572	11.25	98.2
-19	2.1703	0.2445	0.2546	11.26	98.2
-20	2.1724	0.2441	0.2550	11.28	98.4
-21	2.1772	0.2447	0.2556	11.26	98.2
-22	2.1687	0.2440	0.2564	11.25	98.2
averages ± 2σ		0.2444 ± 0.0007		11.25 ± 0.03	98.2 ± 0.2

[redacted]

Table V

Composition of $^{238}PuO_2$ Powder Lot RLN-P-26

Element	ppm by wt.	Element	ppm by wt.
Li	< 0.005	Zn	< 10
Be	< 0.001	Rb	< 0.5
B	< 1	Sr	< 0.1
Na	3	Y	< 0.1
Mg	2	Zr	< 0.1
Al	5	Mo	< 0.5
Si	< 5	Cd	< 0.5
K	2	Sn	< 1
Ca	4	Cs	< 2
Ti	0.2	Ba	< 0.1
V	< 0.5	La	< 1
Cr	< 0.5	Hf	< 0.5
Mn	0.2	Re	< 0.5
Fe	6	Pb	2
Co	< 0.5	Bi	< 1
Ni	4	Am	45
Cu	1		

Pu concentration: Found 88.13% by wt.
Theor. 88.19% by wt.

Table VI

Chemical Analyses of Specimens Shown in Figures 1, 2, and 3

Element	Concentration, ppm by wt. $^{238}PuO_2$	ThO_2-$^{238}PuO_2$	ZrO_2-$^{238}PuO_2$
Li	0.05	< 1	< 1
Be	< 0.002	< 1	< 1
B	< 1	< 1	< 1
Na	11	2	10
Mg	15	10	60
Al	12	500	125
Si	280	200	> 1000 est. M
K	10		
Ca	35	75	
Ti	37		50
V	< 1	< 20	< 30
Cr	6	< 10	< 10
Mn	1	2	< 10
Fe	52	35	300
Co	< 1		
Ni	16	< 5	< 10
Cu	1	25	10
Zn	< 10	10	< 10
Rb	< 1		
Sr	< 0.2		< 3
Y	< 0.2		
Zr	7		
Nb			< 10
Mo	< 1		< 30
Ag			< 1
Cd	< 1	< 5	< 3
Sn	< 3	< 3	< 1
Cs	< 4		
Ba	< 0.1		< 10
La	< 1		
Hf	< 1		
Re	< 1		
Pb	1	< 6	< 3
Bi	< 1	< 2	< 1
^{232}U	0.024		
^{234}U	1240		
Nb	3600		
Am	25		

Table VII

Characteristics of Wafers of ^{238}Pu Materials for Compatibility Test

Composition	Pellet No.	Wt, g	Dia, in.	Length, in.	Immersion Density, g/cc	% Theoretical Density
100% $^{238}PuO_2$	T-12-5-1	0.7730	0.2361	0.1016	10.83	94.5
	-2	0.7760	0.2361	0.1020	10.84	94.6
	-3	0.7735	0.2363	0.1019	10.94	96.5
	-4	0.7707	0.2396	0.0960	10.90	96.0
44 w/o $^{238}PuO_2$-ThO_2	T-12-5-11	0.7642	0.2510	0.1043	9.82	92.9
	-12	0.7704	0.2507	0.1061	9.86	93.2
	-13	0.7681	0.2498	0.1027	9.81	93.7
	-14	0.7677	0.2499	0.1027	9.82	93.8
65 w/o $^{238}PuO_2$-ZrO_2	T-12-5-6	0.7784	0.2496	0.1373	7.54	89.6
	-7	0.7739	0.2490	0.1346	7.62	90.6
	-8	0.7213	0.2491	0.1241	7.57	90.0
	-9	0.7747	0.2497	0.1343	7.57	90.0

Table VIII

Spectrochemical Analysis of Powders Used to Prepare Compatibility Wafers

Element	Concentration, ppm by wt. $^{238}PuO_2$ (Lot WCP-LA-520102)	ZrO_2 (Lot WCP-ZrO_2-1)	ThO_2 (Lot WCP-ThO_2-1)
Li	0.02		< 0.5
Bo	< 0.002	< 1	< 0.5
B	< 1	< 3	0.5
Na	30		20
Mg	40	50	2
Al	55	0.1%	20
Si	40	0.5%	10
K	7		
Ca	70	3.43%	10
Ti	30	100	
V	< 4	50	< 100
Cr	10	50	2
Mn	10	50	< 1
Fe	180	400	20
Co	2	< 30	< 5
Ni	45	10	< 2
Cu	35	30	2
Zn	35	< 30	
Rb	< 4		
Sr	< 0.5		
Y	< 0.5		
Zr	20		
Nb		<300	
Mo	0	<100	
Ag		< 3	
Cd	< 3	< 3	
Sn	70	< 30	
Cs	< 16		
Ba	2		
La	< 8		
Hf	< 4	5, est. 2%	
Re	< 4		
Pb	40	< 30	2
Bi	< 1	< 3	2

Table IX

Comparison of Predicted and Measured Thermal Diffusivity of $^{238}PuO_2$-ZrO_2 Solid Solutions

Temperature, °C	Composition, m/o PuO_2	Thermal Diffusivity, cm^2/sec Predicted[a]	Measured[b]
700	80	0.0090	
700	85		0.0085
1200	80	0.0072	
1200	85		0.0073
700	40	0.0066	
700	45		0.0073
1200	40	0.0037	
1200	45		0.0066

Notes: (a) Data Sheets, LA-4068-MA Appendix, predicted for 5% porosity.
(b) PNL measurements corrected to 5% porosity (tentative).

Table X

Specimens for Thermal Diffusivity Measurements

Specimen No.	Composition	Wt, g	Dia, in.	Length, in.	Geometric Density,[a] g/cc
T-10-144-8	$^{238}PuO_2$	0.2153	0.2439	0.0346	8.13
T-10-144-10	"	0.2120	0.2443	0.0327	8.45
T-10-144-2	ThO_2-44 w/o $^{238}PuO_2$	0.2186	0.2492	0.0340	8.07
T-10-144-3	"	0.2148	0.2521	0.0335	7.84

(a) Based on measured dimensions and weights; true value to be determined after test.

Table XI

True Densities of Companion Specimens Sintered With Thermal Diffusivity Specimens

Specimen No.	Composition	Density g/cc	Density % Theor.
T-10-144-7	$^{238}PuO_2$	10.65	92.9[a]
T-10-144-8	"	10.58	92.4
T-10-144-1	ThO_2-44 w/o $^{238}PuO_2$	9.80	92.7[b]
T-10-144-5	"	9.78	92.4

Notes: (a) Theoretical density = 11.46 g/cc from x-ray analysis
(b) Theoretical density = 10.58 g/cc from x-ray analysis

Table XII

Comparison of Chemical Purity of ThO_2 - 44 w/o $^{238}PuO_2$ Thermal Diffusivity Wafers with that of Starting Powders

Element	Concentration, ppm by wt. $^{238}PuO_2$ (Lot WCP-LA-520102)	ThO_2 (Lot WCP-ThO_2-1)	$^{238}PuO_2$-ThO_2 Sol. Soln.
Li	0.02	< 0.6	< 1
Be	< 0.002	< 0.5	< 1
B	< 1	0.5	< 1
Na	30	20	2
Mg	40	2	10
Al	55	20	500
Si	40	10	200
K	7		
Ca	70	10	75
Ti	30		
V	< 4	< 100	< 20
Cr	10	2	< 10
Mn	10	< 1	2
Fe	180	20	35
Co	2	< 5	
Ni	45	< 2	< 5
Cu	35	2	25
Zn	35		10
Rb	< 4		
Sr	< 0.8		
Y	< 0.8		
Zr	20		
Mo	6		
Cd	< 3		< 5
Sn	70		< 3
Cs	< 16		
Ba	2		
La	< 8		
Hf	< 4		
Pb	< 10	2	< 6
Bi	< 1		< 2

Table XIII

Comparison of Dissolution Rates of $^{238}PuO_2$ Microspheres and $^{238}PuO_2$-ThO_2 Solid Solution Fuel in Sea Water

Sample	Dissolution Rate μg/g/hr	Dissolution Rate μg/sq.mm/hr.
Microspheres	3.9	1.1×10^{-3}
Solid Solution	2.9×10^{-4}	3×10^{-6}
Ratio, Solid Solution / Microspheres	0.74×10^{-4}	2.7×10^{-3}

Table XIV

Specimens Shipped for Safety Tests During Quarter

Date	Receiver	No. Specimens	Type	Purpose
10/8/68	NRDL	4	0.25 in. dia pellets $^{238}PuO_2$-ZrO_2|Y|, 3.5 w/cc	Solubility
10/8/68	Sandia	2	0.25 in. dia pellets ZrO_2|Y|	Small Tunnel Test
"	"	2	2 in. dia discs ZrO_2|Y|	Impact Test
"	"	4	2 in. dia discs with radial hole, ZrO_2|Y|	Large Tunnel Test
10/15/68	NRDL	4	0.25 in. dia pellets $^{238}PuO_2$-ZrO_2|Y| 1.7 w/cc	Solubility
10/16/68	Sandia	6	2 in. dia discs with radial hole, ZrO_2|Y|	Large Tunnel Test
12/6/68	Sandia	3	0.25 in. dia pellets 94% dense $^{238}PuO_2$	Small Tunnel Test

Table XV

Helium Release Results

Expt No.	Temp., °C	D/a^2 min sec^{-1}	D/a^2 max sec^{-1}	Total Fraction released	Time, sec
11637	930	1.8×10^{-7}	2.4×10^{-7}	0.40	80,000
11638	1050	4×10^{-6}	6.3×10^{-6}	0.76	17,600
11639	1232	6×10^{-5}	9.7×10^{-5}	0.95	4,000

PHOTOMICROGRAPHS OF $^{238}PuO_2$ FUEL
(SPECIMEN T-10-91-2, 89.1 % DENSITY)

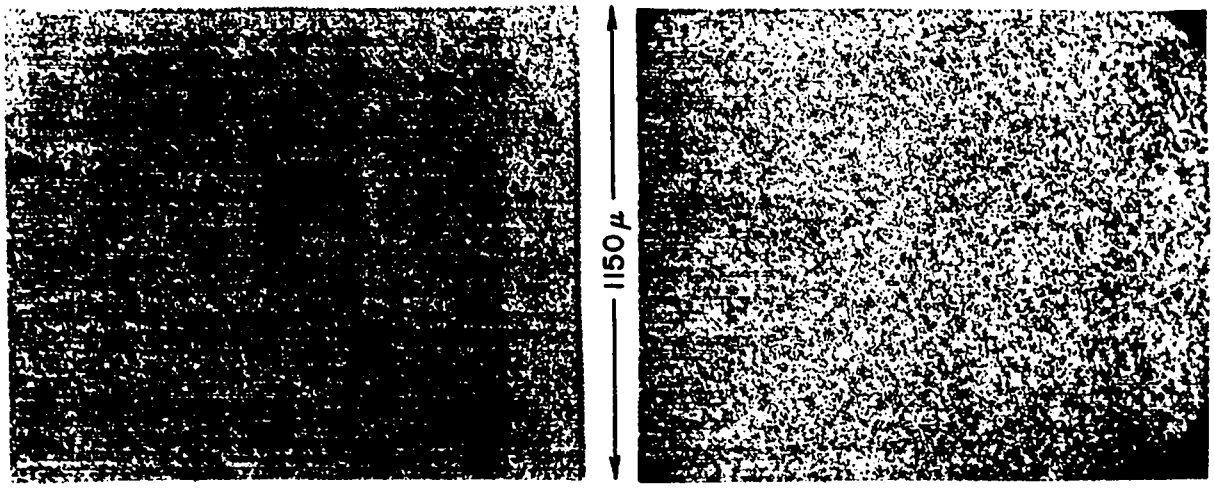

AS POLISHED, 100X

ETCHED, 100X
(10 HCl, 10 HBr, 1 HF, HOT)

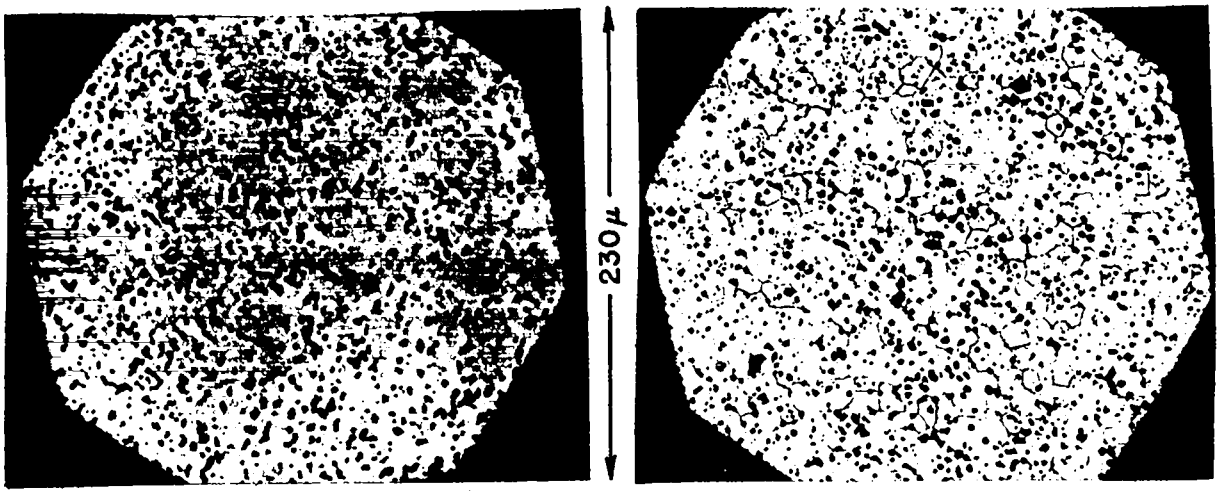

AS POLISHED, 500X

ETCHED, 500X

Figure 1

PHOTOMICROGRAPHS OF $^{238}PuO_2$ - ThO_2 SOLID SOLUTION (SPECIMEN T-10-127-12, 94.5% DENSITY, 44 w/o PuO_2)

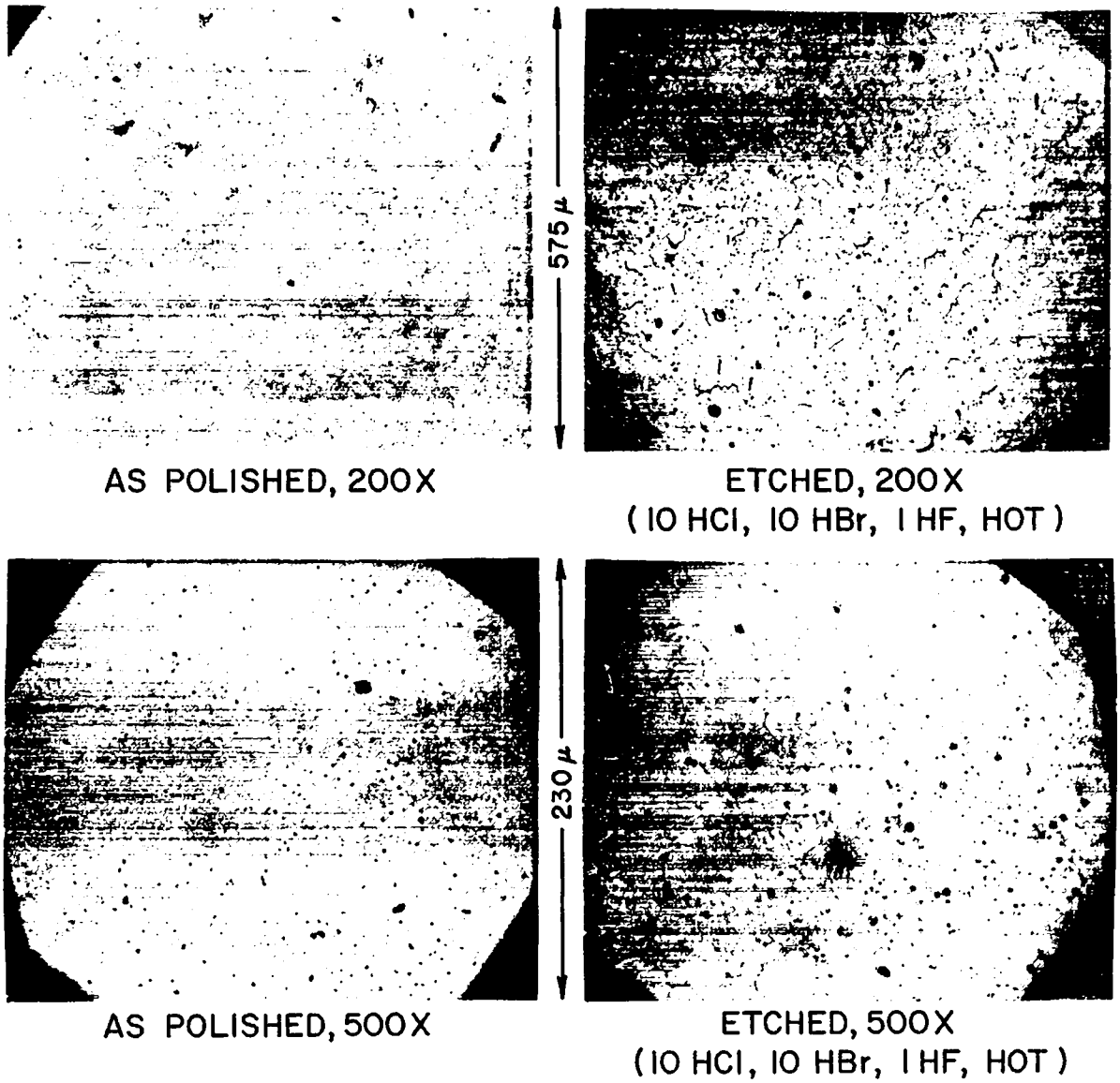

Figure 2

PHOTOMICROGRAPHS OF $^{238}PuO_2$ - ZrO_2 - Y SOLID SOLUTION
(SPECIMEN T-10-120-10, 86.6% DENSITY, 65 w/o PuO_2)

IMPURITY PHASE IN GRAIN BOUNDARY CONTAINS MAINLY Si, Ca, AND O

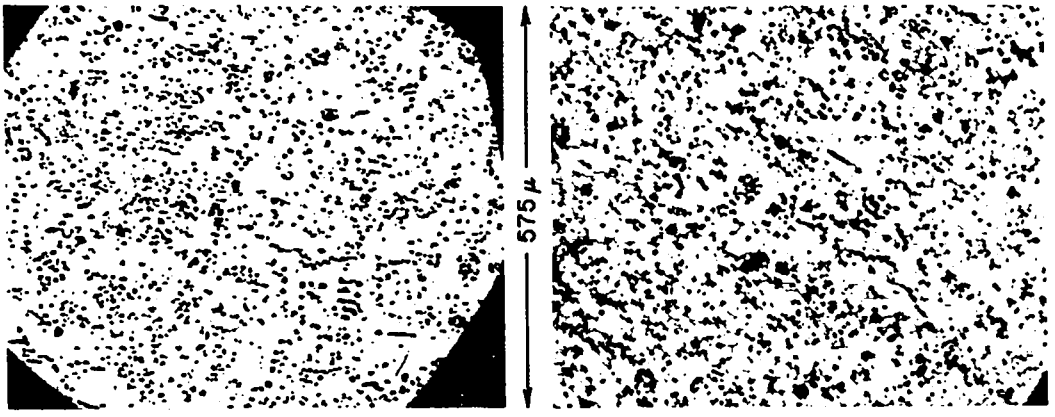

AS POLISHED, 200X

ETCHED, 200X
(10 HCl, 10 HBr, 1 HF, HOT)

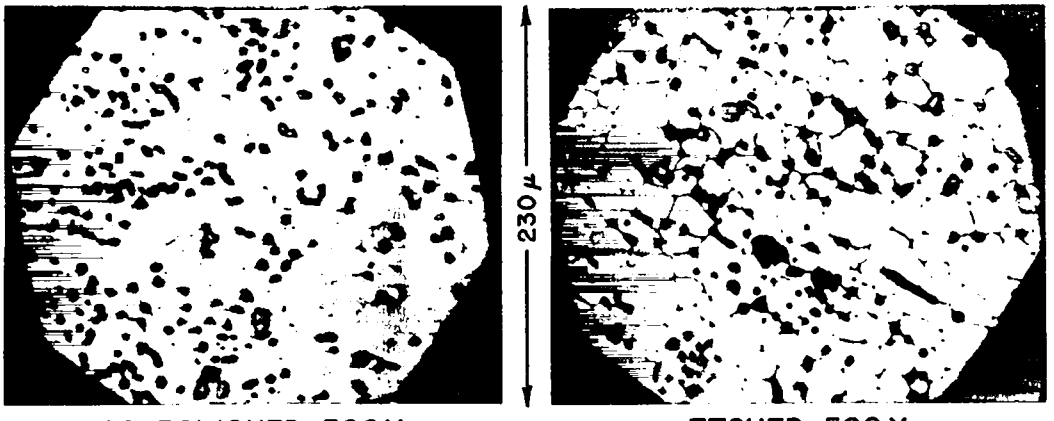

AS POLISHED, 500X

ETCHED, 500X
(10 HCl, 10 HBr, 1 HF, HOT)

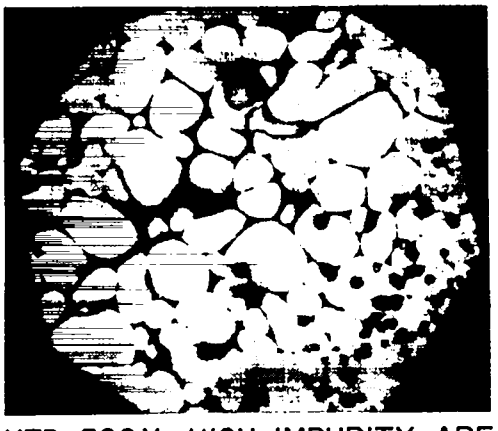

ETCHED 500X - HIGH IMPURITY AREA
(10 HCl, 10 HBr, 1 HF, HOT)

Figure 3

[redacted]

[redacted]

[redacted]

[redacted]